

FATIGUE PROPERTIES OF ADDITIVELY MANUFACTURED TOOL STEEL

C.M. Johnston¹, L.C. Tshabalala¹, and M. Davids²

¹Council for Scientific and Industrial Research (CSIR), Pretoria, South Africa ²University of the Witwatersrand, Johannesburg, South Africa

Abstract

Tool steel is routinely used by the Experimental Aerodynamics group at the Council for Scientific and Industrial Research (CSIR), South Africa, to manufacture critical components for wind tunnel testing. This steel is known for its high strength properties in both tension and compression, and has a good combination of machinability, ductility, and fracture toughness. The emergence of the Additive Manufacturing (AM) technology provides an alternative to traditional manufacturing procedures in the production of wind tunnel model parts and instrumentation; however, use of the AM technology requires knowledge, *inter alia*, of the fatigue characteristics of the AM materials. Test specimens were manufactured from tool steel powder using the Selective Laser Melting (SLM) technology and subjected to fatigue and tensile tests. The thermal treatments were used for stress relieving and aging the additively manufactured part; the processes used in this project were found to have an adverse effect on the properties of the material.

Keywords: Fatigue, Additive Manufacturing, Tool steel

1. Introduction

Additive Manufacturing (AM) can be an efficient method of reducing manufacturing costs, in terms of material wastage, start-up costs, speed, part reduction, and energy usage [1]. In addition, the technology enables the manufacture of complex geometries which may be difficult or impossible to manufacture using conventional techniques. For these reasons, the feasibility of using Additive Manufacturing in the production of wind tunnel components has been explored and implemented at the Council for Scientific and Industrial Research (CSIR) in South Africa. Since high-speed wind tunnel tests are performed in a relatively high-stress environment, it is necessary to understand the fatigue properties of the materials before manufacturing critical parts using AM. Tool Steel is known for its high strength properties and is thus one of the metals routinely used for the manufacture of wind tunnel models and wind tunnel instruments.

M300 Tool Steels have a high alloy content, but virtually no carbon (less than 0.03%). Alloying, together with heat treatment (including age-hardening), produces steels with a combination of high strength, ductility, and fracture toughness. The aged metal contains hard precipitate such titanium carbides (TiC) [2]. The carbon content is therefore kept to a minimum to avoid the formation of TiC precipitates, which would severely reduce the impact strength, ductility, and toughness when present in high concentrations [3].

The yield strengths of 1 500-2 000 MPa after aging is generally acceptable for steels used in aircraft. The rare combination of high strength and toughness found in tool steels makes it well suited especially in safety-critical aircraft structures that require high strength and damage tolerance [3]. In conventionally manufactured M300 tool steels' fatigue limit is lower and usually estimated at 50% of its ultimate tensile strength (UTS) as presented in literature [4]. However, the fatigue limit of M300 tool steels manufactured by additive manufacturing is 20-30% of its UTS which is lower than conventionally engineering materials [4][5][10]. Thus, improving the fatigue limit for the additive

manufacturing part is important especially for the materials used in harsh environments.

In this study, test specimens were produced from a M300 Tool Steel powder and tested for tensile strength and fatigue characteristics. The fatigue strength of M300 is usually expected to exceed one million cycles at approximately 40-60% of its Yield Strength (YS), both in the annealed and aged conditions [8].

2. Test Specimens

The test specimens were manufactured according to the geometry set out in ASTM standard E466 [6]. This standard requires the diameter of the test specimen to be between 5.08mm and 25.4mm, with the cross-sectional area of the grip at least 1.5 times that of the test section, and the length of the test section 2-3 times the length of the test section diameter. The dimensions of the test specimen manufactured are shown in Figure 1.

In this paper, "specimen" shall be used to refer to the Test Specimens as illustrated in Figure 1.

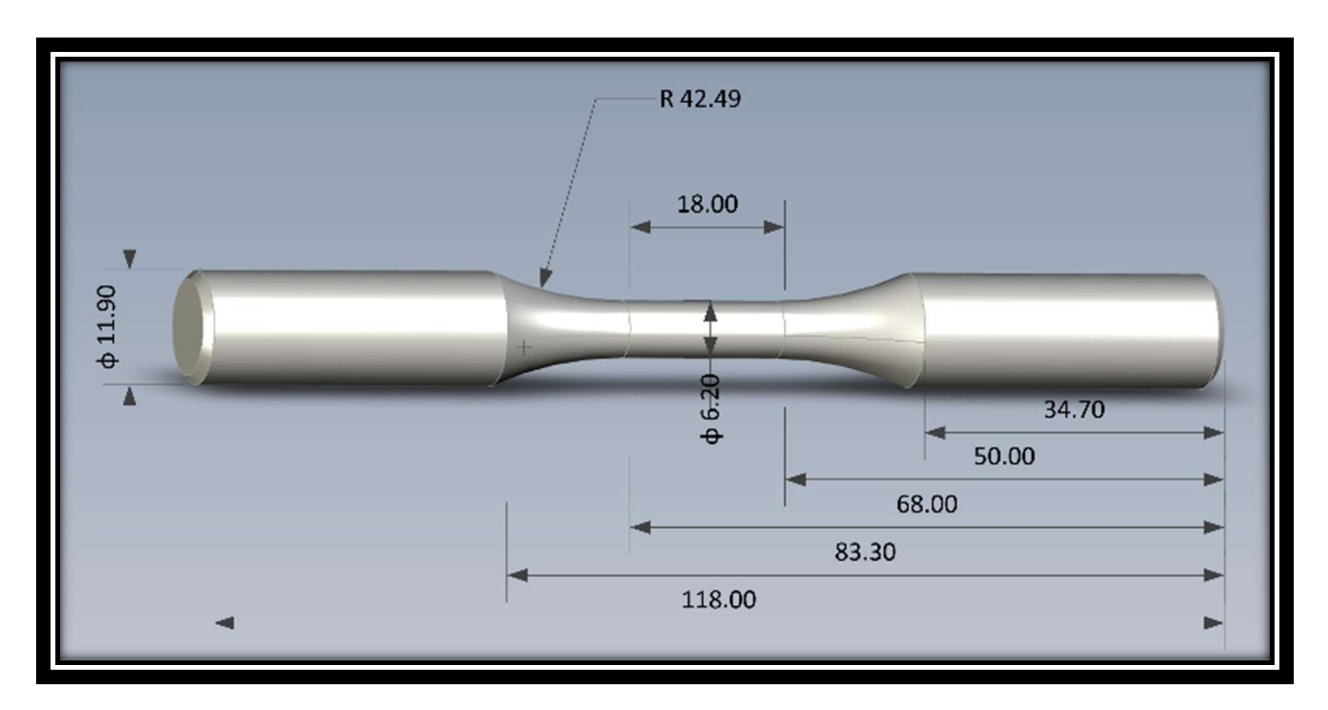


Figure 1 – Test specimen geometry

Thirty test specimens were manufactured on an EOS M280 (Direct Metal Laser Sintering) machine, using metal powder with a particle size distribution of 20– $60~\mu m$. The specimens can be seen in the machine in Figure 2a, from which it can also be seen that the test specimens were manufactured vertically. The scanning strategy was a bi-directional, linear laser movement, with the exposure rotated by 47° between each layer. Solid supports were added around the test specimens during the print, to prevent them from failing. These supports were printed some distance (0.1mm) away from the specimens and fell away from the specimens once they were removed from the baseplate.





Figure 2 – Specimens in the AM machine (a) and in the Testing machine (b)

3. Test Processes

The following procedures were executed on the test specimens.

3.1 Computed Tomography (CT) Scans

Computed Tomography (CT) scans were performed before the specimens were tested. These scans were done on a YXLON FF20 Computed Tomography scanner to investigate any defects in the specimens. The machine parameters for scanning were set to a visibility of \geq 150mm and a frame rate of \leq 58Hz. The open-source software, myVGL was used to read and analyse the CT scan data; the images presented with the discussion in §4.4 used the Edge-detection method.

3.2 Heat Treatment

Two heat treatment procedures were applied:

- **Condition 1** was stress relieving of the specimens at 890°C for 3 hours in accordance with the procedure developed by the machine operator [7], and then left to cool in the furnace. This was done before the specimens were removed from the base plate.
- Condition 2 was performed on specimens which were in Condition 1 and was thermal aging of the specimens at 480°C for 3 hours, after which the specimens were left to cool at room temperature.

3.3 Tensile and Fatigue tests

An Instron Model 1342 servo-hydraulic universal testing machine was used for the tensile and fatigue tests (Figure 2b). The tension-tension fatigue tests were run between 10 and 15 Hz, corresponding to High Cycle Fatigue testing. The fatigue was carried out as tension-tension test at a R-ratio of 0.1.

The results of these tests are presented in §4.1 and §4.2.

3.4 Fracture analysis using SEM

When the tests yielded unexpected results, a Jeol JSM-6010PLUS Microscope was used to analyse the surface fractures of specimens; this is discussed in §4.3.

3.5 Mass Spectrometry

As part of the investigation into the unexpected results, a mass spectrometry test was performed on one test specimen; this is discussed in §4.3.

4. Results and Discussion

The fatigue tests performed on the AM parts (discussed below) generated results which were not consistent with the specifications of the AM powder used in this project. In an effort to determine the source of the anomaly, a number of additional tensile tests were performed for the specimens in the two Conditions, fractography was performed, and a mass spectrometry test was executed.

4.1 Tensile Tests

Tensile tests were run on five of the test specimens, to compare the material properties to those specified for the powder. The tensile test results are given in Table 1 for two specimens in Condition 1, and in Table 2 for three specimens in Condition 2 (refer §3.2).

The specimens which were stress relieved in the austenite phase region but not aged (Condition 1, Table 1) had:

- YS slightly lower than the specification but on average within the uncertainty band,
- UTS marginally higher than the specification, and within the uncertainty band,
- Elongation less than the specification and outside the uncertainty band.

Specimen ID	Ultimate Tensile Stress [MPa]	Yield [MPa]	Elongation [%]	Diameter [mm]
AM Powder Spec	1 100	990	15	6.35 nominal
	± 100	± 100	± 5	
06 - HT	1 192	917	8.04	6.10
07 - HT	1 192	878	6.54	6.11
Mean	1 192	898	7.29	6.11

Table 1 - Tensile tests results: Condition 1 (HT)

The specimens which were stress relieved and aged (Condition 2, Table 2) had:

- Low YS, this being largely unchanged from the un-aged specimens (results were only obtained from one specimen),
- UTS which, while higher that the un-aged specimens, achieved only approximately half to the expected increase in strength,
- No elongation.

Table 2 - Tensile tests results: Condition 2 (HT and A)

Specimen ID	Modulus [GPa]	Ultimate Tensile Stress [MPa]	Yield [MPa]	Elongation [%]	Diameter [mm]
AM Powder Spec	-	2 105	2 100	2	-
23 - A	191	1 497	-	0.17	6.13
02 - A	195	1 489	1 026	0.46	6.11
01 - A	193	1 709	-	0.13	6.12
Mean	193	1 565	1 026	0.25	6.12
Standard Dev	2.1	125	-	0.18	0.01

4.2 Fatigue Testing

The fatigue tests were planned with numerous test specimens, which were to be tested in Condition 2. However, once the tests produced unanticipated results, some of the test specimens were diverted for more tensile tests, and tests in Condition 1.

High-cycle fatigue tests were limited to the 2.5 million cyclic stress range. The test conditions for the fatigue tests are noted in §3.3 and the results of the tests are presented in Table 3 and Figure 3.The fatigue test results in Table 3 provide details on the applied loads and observed fatigue life.

Table 3 - Fatigue tests results: Condition 2 (HT and A)

Gauge Diameter [mm]	Area [mm²]	Max Stress [MPa]	Max Loading [kN]	Stress Amplitude [MPa]	Cycles to failure
6.16	29.80	211	6.30	53	2 479 792 (runout)
6.05	28.75	299	8.61	135	170 269
6.15	29.71	299	8.89	135	395 275
6.12	29.42	423	12.43	190	44 692
6.08	29.03	563	16.36	254	19 937
6.16	29.08	704	20.99	317	4 200
6.16	29.80	986	29.38	503	1 413
6.14	29.61	1 170	34.64	527	2 879
6.17	29.90	1 170	34.98	526	5 658

A S-N curve was used to represent the data, see Figure 3. Scatter was noted in the data at the higher loads. The outcome of the material fatigue trend is lower but comparable to results in literature for Z-direction printed, stress relieved specimens [10]. This indicates that the thermal ageing used in the project had an adverse effect on the properties of the material.

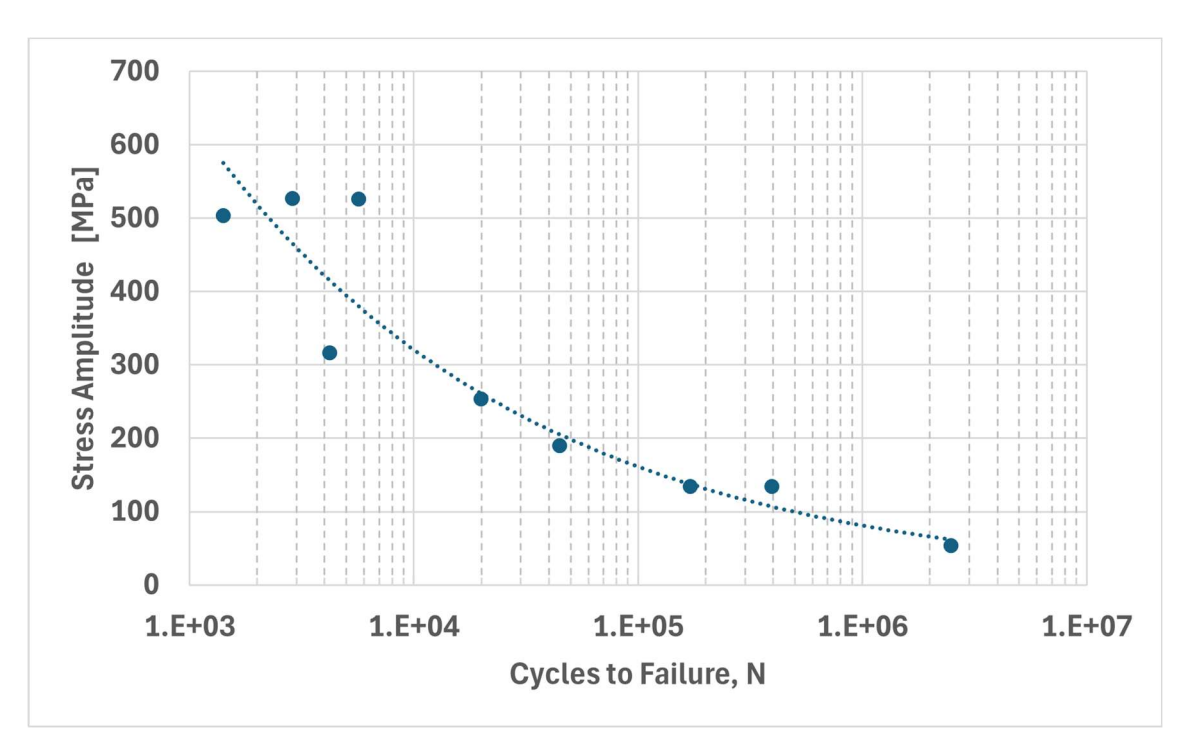


Figure 3 – S-N curve for aged AM Tool Steel

4.3 Fractography

Specimen 18, which was fatigue tested at a Stress Amplitude of 527 MPa (~80% of the YS), failed after 2 879 cycles. The fracture surface of Specimen 18 displays stress raisers (see Figure 4), and it appears that crack initiation did occur near the surface (see Figure 5a). There are no beach marks on the specimens investigated, to suggest a smooth, ductile failure and so a brittle failure was deduced.



Figure 4 – Fractured surface of Specimen 18

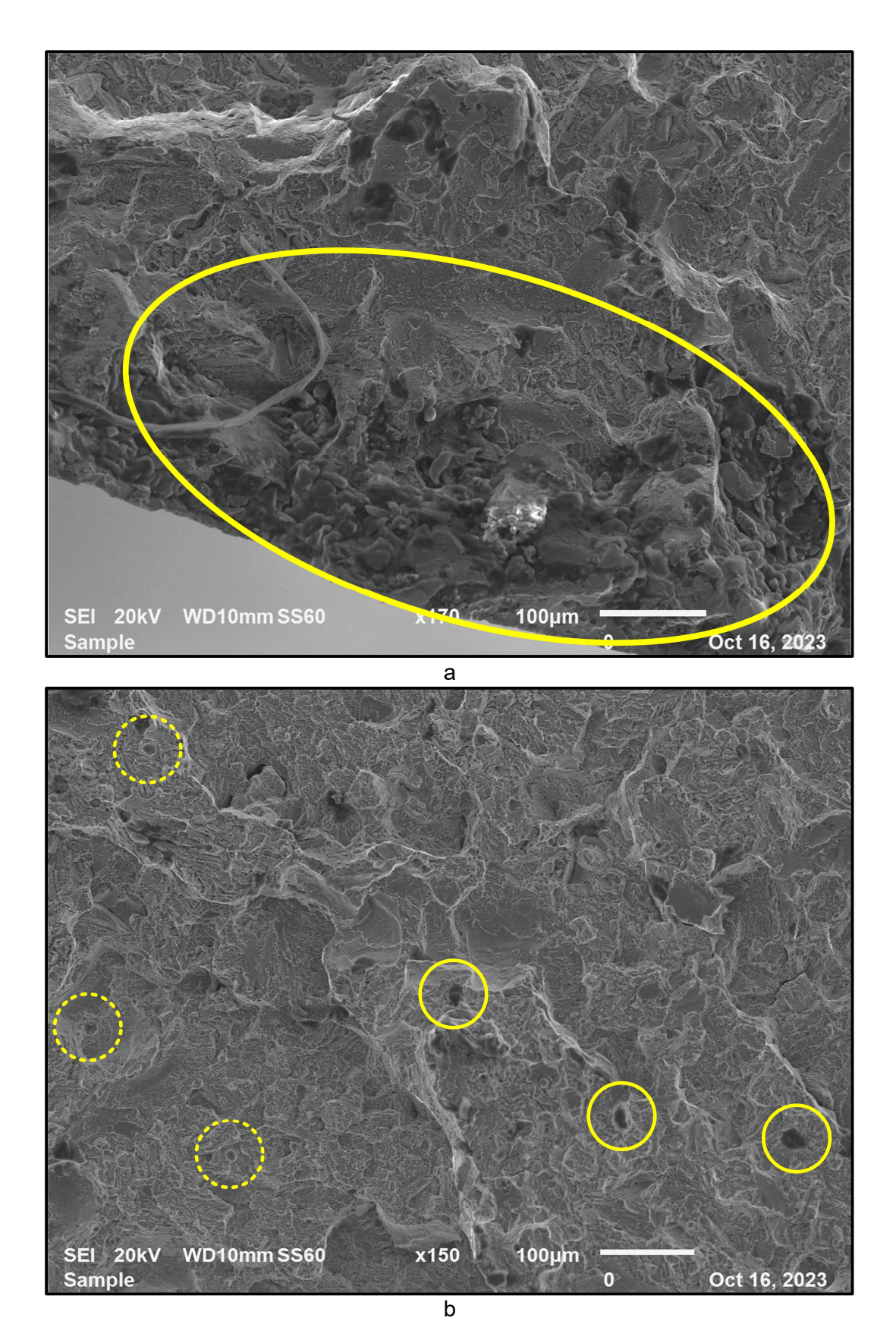


Figure 5 – Micrographs of Specimen 18

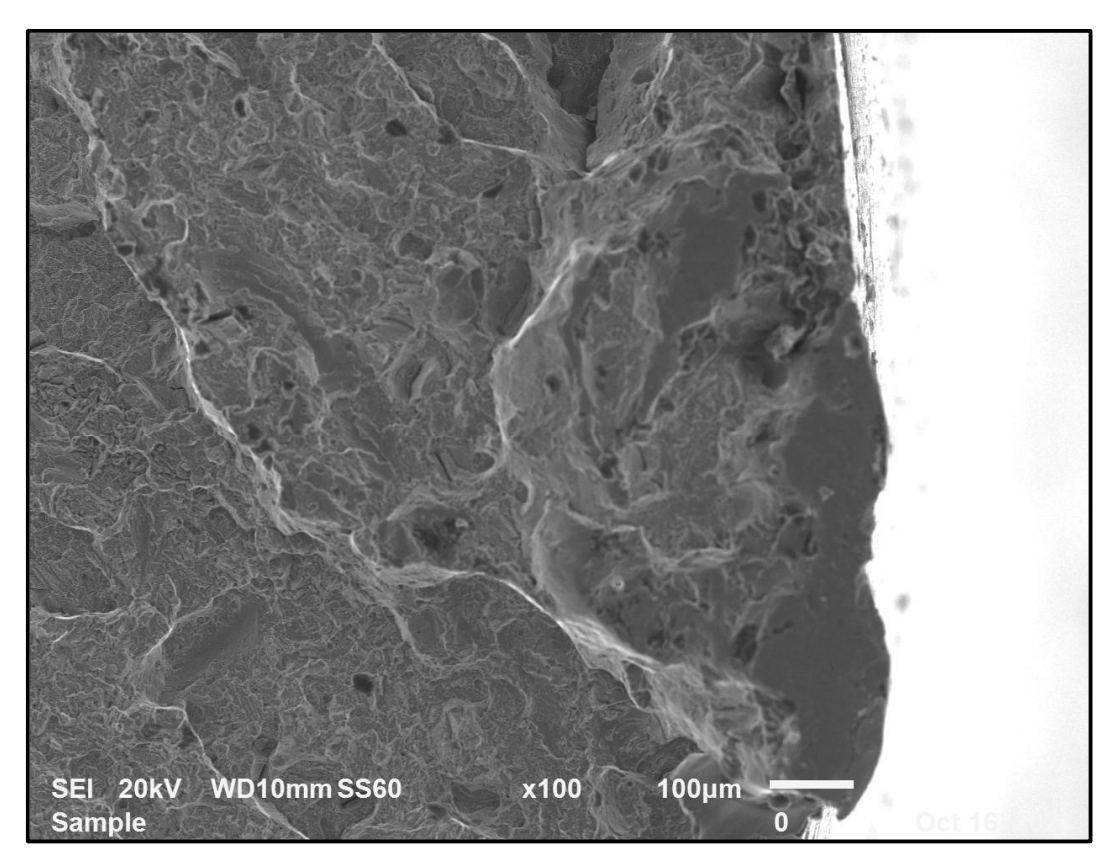


Figure 6 – Micrograph of edge of Specimen 18

In Figure 5b and Figure 6 the specimen shows defects, especially along the outer edges on the surface that correlates to a feature of Additive Manufacturing known as keyhole porosity. The keyhole is a phenomenon that occurs when material is quickly melted and forms a cavity. It is then possible for gas to be trapped within this cavity after solidification. A study has shown that this keyhole porosity is more likely to occur whenever the laser changes direction, i.e. reaches a point of zero velocity [12].

The micropores in the inner structure are visible and highlighted with the rings in Figure 5b. This is likely due to gas and keyhole porosity effects, where gas porosity is characterised by spherical shapes (dashed circles) and keyhole porosity (solid circles) is more irregularly shaped (see Figure 5b) [12]. The last point of contact is indicated by the flat surface seen in Figure 6. This is the point where the specimen snapped apart completely at failure.

4.4 Computed Tomography (CT) Scans

The CT scans were performed on the test specimens, in both Conditions to obtain visualisation of the internal structure of the laser AM processed specimens. The effect of the internal structure on the fatigue results could then be determined. This scanning technique is capable of detecting and qualifying voids or defects in the specimen interior. [9]. The horizontal cross-sections of the gauge length of the specimen were imaged at the points specified in Figure 7, with extracts of the scans presented in Figure 8.

The CT scan data for specimen 18 before and after aging is shown in Figure 8. From the variation in the scans in both conditions, it appears that the aging process improved the features near the surface of the specimen and reduced detected internal features, without eliminating them entirely. The existence of surface defects has a negative impact on mechanical properties, as they can decrease a material's tensile strength and fatigue resistance [11].

It is important to note that, depending on the scan quality (the presence of artefacts, noise, image

blur, etc), the de-noising techniques used and analysis workflow used in image processing, different results can be obtained [9]. These can also be presented in different ways which may lead to misinterpretation [9]. From the scans presented it is not completely clear whether the detected edge features are voids or known AM defects.

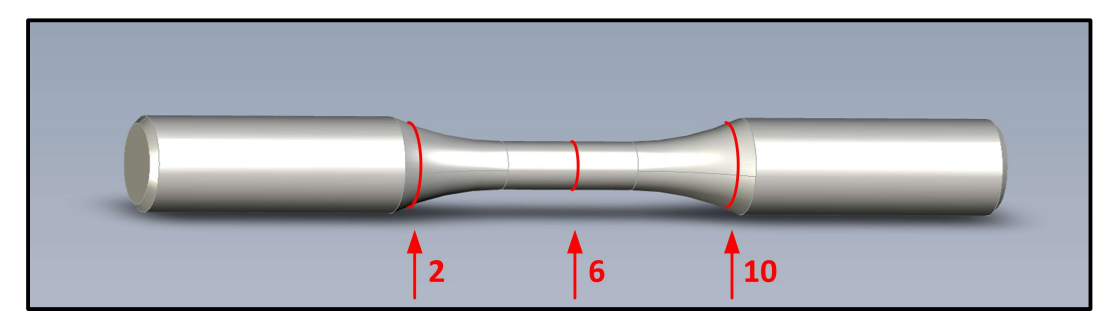
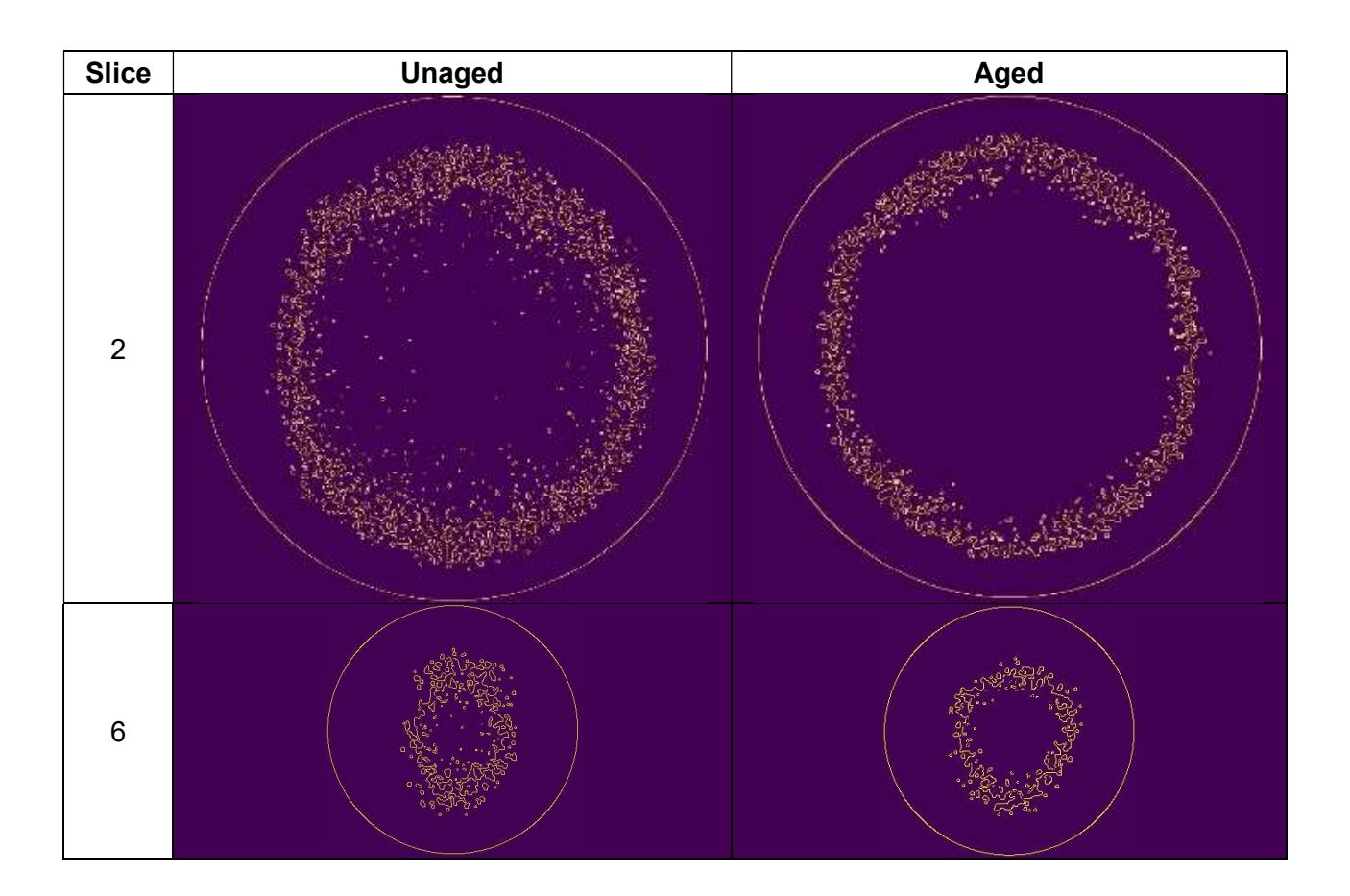


Figure 7 – Location of the CT scans presented in Figure 8



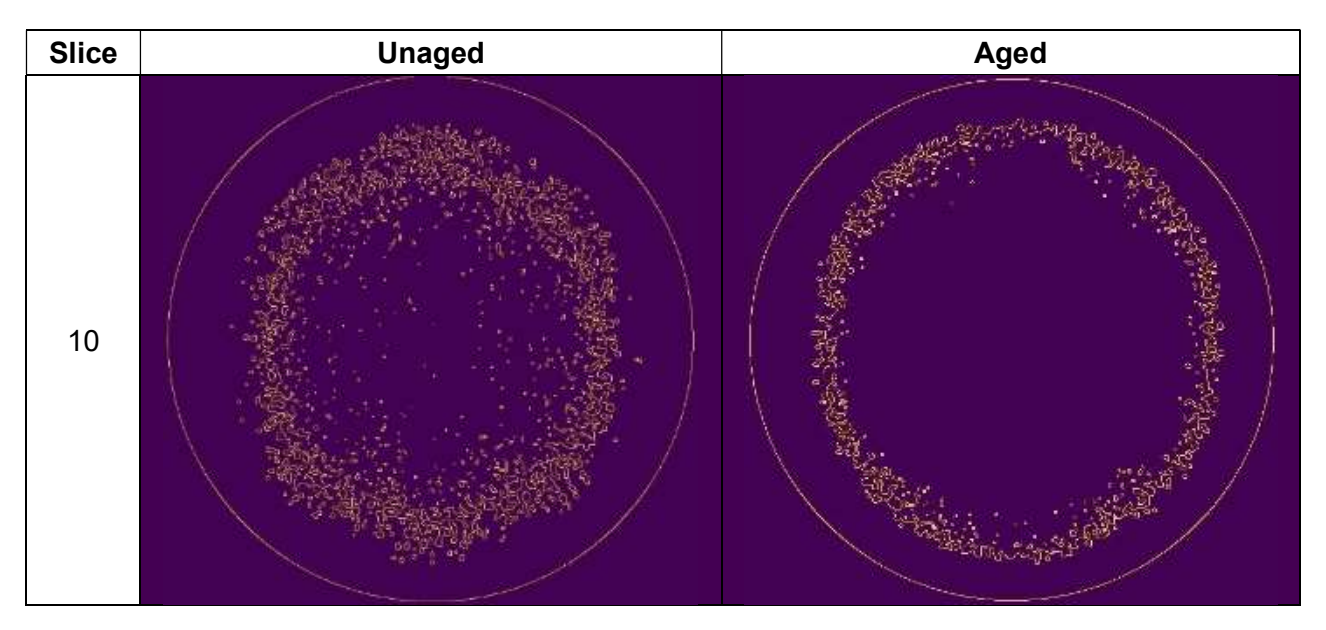


Figure 8 – CT Scans of Specimen 18 at various locations, before (a) and after aging (b)

4.5 Mass Spectrometry

The results, presented in Table 4, indicated that the elements were within specification, apart from the Ti which was high. The higher levels of Ti could make the possibility of TiC precipitates plausible. Due to the high alloying contents of Ni, Co and Mo, the other types of precipitates formed would include Ni3Mo, Ni3Ti, Ni3Al and Fe2Mo, can occur in a high-volume fraction after aging. Cobalt is used to reduce the solubility limit of molybdenum and thereby increase the volume fraction of Mo-rich precipitates (e.g. Ni3Mo, Fe2Mo). The precipitates promote strengthening by the precipitation hardening process through thermal aging [10],[11]. The results obtained in this project indicate loss of plasticity, as well as a decrease in elongation from 7.29% in HT condition to 0.25% after aging, this can be attributed to the precipitates formed.

Table 4 – Comparison of measured to expected composition, for Specimen 2 (Condition 1, HT)

Element	M300	Powder Specification	Specimen 2
Fe	Bal	Bal	Bal
Ni	18.36	17.0-19.0	17.12
Co	8.77	8.0-11.0	9.53
Мо	5.06	4.5-5.2	5.2
Ti	0.59	0.3-1.2	1.69
С	0.007	0.03 max	0.01
Al	0.1	0.15 max	0.138
Cr	0	0.5 max	0.13
Si	0.02	0.1 max	0.08
Mn	0.01	0.1 max	0.03
Р	0.004	0.03 max	0.014
S	0.002	0.01 max	0.005
Cu	-	-	0.01
V	0	-	0.005
В	-	-	0.0024
Nb	0	-	0.02

5. Conclusion

Annealing followed by ageing caused a significant under-performance in the UTS of the additively manufactured Tool Steel specimens, compared to the published AM specifications. However, the results for specimens which were only stress-relieved and not aged, exhibited properties comparable to the specifications.

After investigating various potential sources for this anomaly, it was deduced that the use of both thermal processes had unfavourable effect on the tensile properties of the specimens. These properties then affected the results of the fatigue tests.

A S-N curve was generated for the aged Tool Steel. The run-out stress was achieved at about 200 MPa, which is ~15% of the aged YS.

Further investigation is underway into the effects of and best practice for thermal treatment of AM Tool Steel.

6. Contact Author Email Address

Mailto: cjohnsto@csir.co.za

7. Acknowledgements

The authors would like to acknowledge and thank the South African Air Force (SAAF) and the Armaments Corporation of South Africa (ARMSCOR) for their support of this project.

8. Copyright Statement

The authors confirm that they, and/or their company or organization, hold copyright on all of the original material included in this paper. The authors also confirm that they have obtained permission, from the copyright holder of any third-party material included in this paper, to publish it as part of their paper. The authors confirm that they give permission, or have obtained permission from the copyright holder of this paper, for the publication and distribution of this paper as part of the ICAS proceedings or as individual off-prints from the proceedings.

References

- [1] Wohlers TT, Campbell RI, Diegel O, Huff R, Kowen J. Wohlers Report 2023: 3D Printing and additive manufacturing: Global state of the industry, Wohlers Associates, 2023.
- [2] Pérez-Gonzalo I, González-Pociño A, Alvarez-Antolin F, and del Rio-Fernández L. Analysis of a double aging process in a maraging 300 steel fabricated by selective laser melting, using the design of experiments technique in metals, Vol. 13, 2023.
- [3] Mouritz AP. *Introduction to aerospace materials*, Chapter 11: Steels for aircraft structures, pp. 232–250, Woodhead Publishing, 2012.
- [4] Croccolo D., De Agostinis M., Fini S., Olmi G., Vranic A., Ciric-Kostic S. *Influence of the build orientation on the fatigue strength of EOS maraging steel produced by additive metal machine*, Fatigue Fract. Eng. Mater. Struct., Vol. 39 (5), pp. 637–647, 2016, doi:10.1111/ffe.12395.
- [5] Croccolo N., De Agostinis M., Fini S., Olmi G., Vranic A., Ciric-Kostic S., Sensitivity of direct metal laser sintering Maraging steel fatigue strength to build orientation and allowance for machining, Fatigue Fract. Eng. Mater. Struct., Vol. 42 (1), pp. 374–386, 2019, doi: 10.1111/ffe.12917.
- [6] ASTM International Standard practice for conducting force controlled constant amplitude axial fatigue tests of metallic materials, ASTM E466-15, 2018 Annual Book of ASTM Standards, Vol. 03.01, 2018.
- [7] Adam I, du Preez WB, Combrinck J. Stress relieving of maraging steel injection mould inserts built through additive manufacturing, RAPDASA 2017 Conference Proceedings, pp. 1-10, 2017.
- [8] Tshabalala L, Sono O, Makoana W, Masindi J, Maluleke O, Johnston C, Masete. S Axial fatigue behaviour of additively manufactured tool steels, Materials Today: Proceedings, Vol. 38, Part 2, pp. 789-792, 2021. ISSN 2214-7853.
- [9] du Plessis A, Sperling P, Beerlink A, Tshabalala L, Hoosain S, Mathe N, le Roux SG. Standard method for microCT-based additive manufacturing quality control 1: Porosity analysis, MethodsX, Vol. 5, pp. 1102-1110, 2018.
- [10]Raju N, Rosen DW. Fatigue properties of 3d printed maraging steel, Proceedings of the 32nd Annual International

- Solid Freeform Fabrication Symposium, 2021.
- [11]Raghuraman V. and Sampath T. Influence of in-situ process parameters, post heat treatment effects on microstructure and defects of additively manufactured maraging steel by laser powder bed fusion—A comprehensive review, Physica Scripta, Vol. 99 (5), 2024, DOI 10.1088/1402-4896/ad3681
- [12] Mostafaei A. et al. *Defects and anomalies in powder bed fusion metal additive manufacturing*, Current Opinion in Solid State and Materials Science, Vol. 26, 2022.